Morphotropic Phase Diagram and Dielectric and Ferroelectric Properties of $(1-x)Ba(Sc_{1/2}Nb_{1/2})O_3-xPbTiO_3$ Solid Solution

Qian Wei,[†] Zujian Wang,[†] Xiuzhi Li,[†] Xifa Long,*[,†] and Zuo-Guang Ye*[,‡]

Key Laboratory of Optoelectric Materials Chemistry and Physics, Fujian Institute of Research on the Structure of Matter, Chinese Academy of Sciences, Fuzhou, Fujian 350002, China, and Department of Chemistry and 4D Laboratories, Simon Fraser University, 8888 University Drive, Burnaby, British Columbia, V5A IS6, Canada

Received October 8, 2008. Revised Manuscript Received December 15, 2008

The solid solution of $(1-x)Ba(Sc_{1/2}Nb_{1/2})O_3-xPbTiO_3$ ($0 \le x \le 1$) has been synthesized in the perovskite structure by solid-state reaction in the form of ceramics and characterized by means of X-ray diffraction, dielectric spectroscopy, and ferroelectric measurements. A partial solid-state phase diagram ($T \approx x$) of the binary system is established based on the X-ray and dielectric measurement. A morphotropic phase boundary (MPB) region is found within the composition range of $x = 0.61-0.65$. The dielectric permittivity is enhanced greatly by increasing the PT content, reaching peak values for the MPB compositions. The ceramics of 0.42BSN-0.58PT show typical relaxor ferroelectric behavior with diffuse maxima of permittivity, which shift to higher temperatures when increasing the frequency. With further increase in PT amount, the dielectric permittivity peaks become sharper and frequency independent, indicating a ferroelectric phase transition, the Curie temperature (T_c) of which increases accordingly. The change in dielectric properties reveal the transformation from dielectric to relaxor and to ferroelectric behavior, induced by composition in the solid-solution system.

1. Introduction

Lead-based relaxor ferroelectrics with complex perovskite structure have attracted much attention because of their extensive applications in multilayered ceramic capacitors,[1] electrostrictive actuators, and micropositioners.[2,3] Many relaxor ferroelectrics form binary solid-solution systems with lead titanate $PbTiO_3$, a typical ferroelectric, for example, $Pb(Mg_{1/3}Nb_{2/3})O_3-PbTiO_3$ (PMN-PT), $Pb(Zn_{1/3}Nb_{2/3})O_3-PbTiO_3$ (PZN-PT), and $Pb(Sc_{1/2}Nb_{1/2})O_3-PbTiO_3$ (PSN-PT).[4−6] An interesting phenomenon is that the so-called morphotropic phase boundary (MPB) exists in all these solid-solution systems and the excellent piezoelectric properties occur in those compositions close to or within the MPB region. The term MPB was first proposed by Jaffe et al.[7] in the $Pb(Zr_{(1-x)}Ti_x)O_3$ (PZT) solid-phase diagram to separate rhombohedral phase from tetragonal phase. Following this original work, the MPB has been found in many other solid solution systems. More recently, a new phase of monoclinic or orthorhombic phase has been discovered in the MPB regions of the PZT,[8] PMN-PT,[9−13] PZN-PT,[14,15] and PNN-PT[16] systems, which bridges the rhombohedral and tetragonal phases. Interestingly, outstanding dielectric and piezoelectric properties are found near or within the MPB regions, making these materials excellent candidates for such applications as multilayered capacitors, electromechanical sensors and actuators, and ultrasonic imaging probes.

As typical relaxor-based solid-solution materials, PMN-PT and PZN-PT single crystals have received much attention in the sense that their superior piezoelectric properties and the physics and chemistry of their MPBs have been extensively investigated. However, because of the high lead content in the composition, these materials have raised significant environmental concerns. Therefore, a great deal of efforts have been put in searching for lead-free and lead-reduced materials with high Curie temperature and good piezoelectric performance, with a view of replacing the lead-based piezo-/ferroelectrics. One of the generally used approaches was to substitute the Pb^{2+} ions with the Bi^{3+} or Ba^{2+} ions.[17−22] Recently, we reported a lead-reduced ferro-

* Corresponding author. Phone: (86)-591-83710369(X.L.); (778) 782-8064 (Z.-G.Y.). Fax: (86)-591-83714946 (X.L.); (778) 782-3765 (Z.-G.Y.). E-mail: lxf@fjirsm.ac.cn (X.L.); zye@sfu.ca (Z.-G.Y.).

[†] Chinese Academy of Sciences.

[‡] Simon Fraser University.

(1) Yamashita, Y. *Am. Ceram. Soc. Bull* **1994**, *73*, 8.
(2) Cross, L. E.; Jang, S. J.; Newnham, R. E.; Nomura, S.; Uchino, K. *Ferroelectrics* **1980**, *23*, 187.
(3) Uchino, K. *Ferroelectrics* **1994**, *151*, 321.
(4) Choi, S. W.; Shrout, T. R.; Jang, S. J.; Bhalla, A. S. *Ferroelectrics* **1989**, *100*, 29.
(5) Kuwata, J.; Uchino, K.; Nomura, S. *Ferroelectrics* **1981**, *37*, 579.
(6) Bing, Y.-H.; Ye, Z.-G. *J. Cryst. Growth* **2006**, *287*, 326.
(7) Jaffe; B.; Cook; W. R.; Jaffe; H. *Piezoelectric Ceramics*; Academic Press: London, 1971.
(8) Noheda, B.; Cox, D. E.; Shirane, G. *Appl. Phys. Lett.* **1999**, *74*, 2059.
(9) Park, S. E.; Shrout, T. R. *J. Appl. Phys.* **1997**, *82*, 1804.
(10) Choi, S. W.; Shrout, T. R.; Jang, S. J.; Bhalla, A. S. *Mater. Lett.* **1989**, *8*, 253.
(11) Noheda, B.; Cox, D. E.; Shirane, G.; Gao, J.; Ye, Z.-G. *Phys. Rev. B* **2002**, *66*, 054104/1.
(12) Bokov, A. A.; Ye, Z.-G. *J. Appl. Phys.* **2004**, *95*, 6347.
(13) Ye, Z.-G.; Bing, Y.; Gao, J.; Bokov, A. A.; Stephens, P.; Noheda, B.; Shirane, G. *Phys. Rev. B* **2003**, *67*, 104104/1.
(14) Kuwata, J.; Uchino, K.; Nomura, S. *Ferroelectrics.* **1981**, *37*, 579.
(15) La-Orauttapong, D.; Noheda, B.; Ye, Z.-G.; Gehring, P. M.; Toulouse, J.; Cox, D.; Shirane, G. *Phys. Rev. B* **2002**, *65*, 144101/1.
(16) Chung, S. T.; Nagata, K.; Igarashi, H. *Ferroelectrics* **1989**, *94*, 243.
(17) Chen, M.; Xu, Q.; Kim, B. H.; Ahn, B. K.; Ko, J. H.; Kang, W. J.; Nam, O. J. *J. Euro. Cera. Soc.* **2008**, *28*, 843.

10.1021/cm802734n CCC: $40.75
Published on Web 01/15/2009

electric solid solution of $(1-x)Ba(Mg_{1/3}Nb_{2/3})O_3-xPbTiO_3$, which also exhibits an MPB region within the composition range of 70−73 mol % PT and shows a Curie temperature above 200 °C.[23] As a member of complex perovskite $A(B'B'')O_3$, $Ba(Sc_{1/2}Nb_{1/2})O_3$ (BSN) has received relatively little attention. Politova et al. reported preliminary study of the dielectric properties of the $(1-x)Ba(Sc_{1/2}Nb_{1/2})O_3-xPbTiO_3$ solid solution.[24] However, the phase relationship and other properties, such as ferroelectric properties, remain to be investigated more thoroughly. In this paper, we report the synthesis, phase analysis and dielectric and ferroelectric characterizations of the ceramics of the $(1-x)Ba(Sc_{1/2}Nb_{1/2})O_3-xPbTiO_3$ solid solution. The solid-state phase diagram of the system has been established, which reveals the existence of a morphotropic phase boundary region where the dielectric properties are enhanced.

2. Experimental Section

The ceramics of the $(1-x)Ba(Sc_{1/2}Nb_{1/2})O_3-xPbTiO_3$ solid solution, with the compositions of $x = 0$, 0.4, 0.5, 0.53, 0.58, 0.60, 0.61, 0.62, 0.63, 0.64, 0.65, 0.66, 0.67, 0.70, and 0.80, were synthesized by solid state reaction. High purity (>99.99%) chemicals of $BaCO_3$, Sc_2O_3, Nb_2O_5, TiO_2, and PbO were used as the starting materials. First, the starting materials were weighed in stoichiometric proportions and wet-mixed. After mixing and drying, the pressed pellets were calcined at temperatures around 1100−1160 °C for 4 h. Second, the calcined powders were reground and pressed into pellets and sintered at 1320−1380 °C for 2.5 h in a sealed Al_2O_3 crucible to form the series of desired ceramics.

For structural analysis, X-ray diffraction was performed at room temperature on a Rigaku diffractometer (DMAX2500) equipped with Cu Kα radiation and a graphite monochromator. The data were collected with a scan step of 0.02° (2θ) and an angular range of 10−80°. The dielectric properties were measured using a computer-controlled Alpha dielectric/impedance spectrometer (NovolControl, Germany) at a field of 0.5 V_{rms}. The measurements were carried out as a function of temperature upon heating from −150 to 300 °C. A TF 2000 Analyzer (aixACCT) standard ferroelectric testing system was used to display the polarization-electrical field ($P-E$) hysteresis loops.

3. Results and Discussion

3.1. X-ray Diffraction. The XRD patterns of the BSN-PT ceramics with selected compositions of $0.55 \le x \le 0.70$ are presented in Figure 1. It shows that all the ceramic samples exhibit a pure phase of perovskite structure. At compositions with $x = 0.66$ and higher, the (100), (110), (200), (210), and (211) reflection peaks become gradually broadened and then clearly split into two peaks with increasing PT content, which indicates a tetragonal symmetry. At composition with $x = 0.61$, the (200), (210), and (211) reflection peaks undergo an asymmetrical broadening,

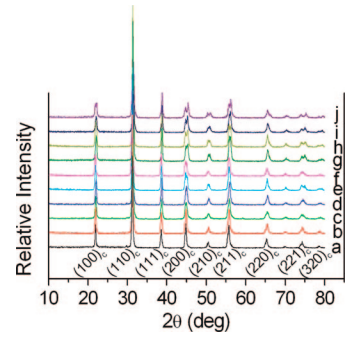

Figure 1. XRD patterns of the $(1-x)Ba(Sc_{1/2}Nb_{1/2})O_3-xPbTiO_3$ ceramics with selected compositions. (a) $x = 0.55$, (b) $x = 0.58$, (c) $x = 0.60$, (d) $x = 0.61$, (e) $x = 0.62$, (f) $x = 0.63$, (g) $x = 0.64$, (h) $x = 0.65$, (i) $x = 0.66$, (j) $x = 0.70$.

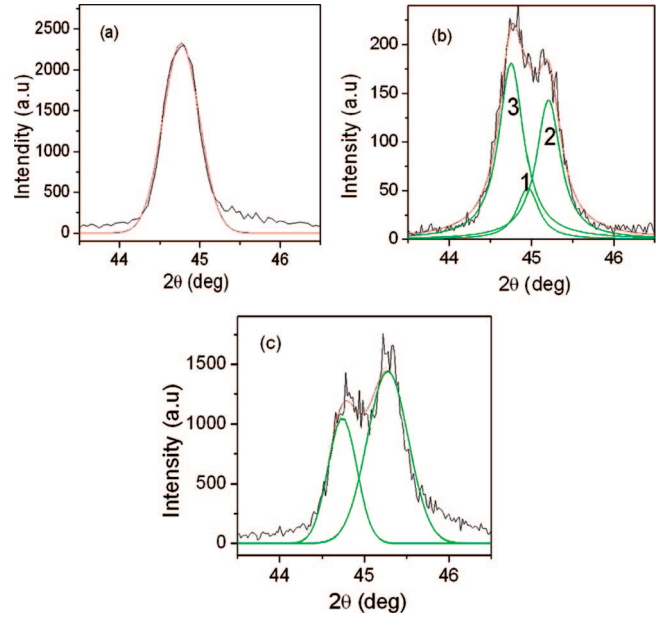

Figure 2. Pseudocubic (200) reflection peaks in the interval of $2\theta = 43.5-46.5°$ for the compositions of $(1-x)Ba(Sc_{1/2}Nb_{1/2})O_3-xPbTiO_3$: (a) $x = 0.60$, (b) $x = 0.62$, and (c) $x = 0.66$, with deconvolutions of the rhombohedral and tetragonal symmetry.

indicating the coexistence of rhombohedral and tetragonal phases. Furthermore, a gradual transformation from rhombohedral to tetragonal phase can be observed with the PT concentration increasing from $x = 0.50$ to $x = 0.70$.

Figure 2 shows the pseudocubic (200) reflection peaks in the angle interval of $2\theta = 43.5-46.5°$ for compositions with $x = 0.60$, 0.62, and 0.66. For $x = 0.60$, the (200) reflection is composed of only one single peak, corresponding to the rhombohedral phase. For $x = 0.62$, the (200) reflection is composed of three peaks. The dominant peak 3 corresponds to the residual rhombohedral phase and peaks 1 and 2 represent the tetragonal phase. For $x = 0.66$, the distinct split of (200) reflection and the completely vanished rhombohedral peak indicate the tetragonal symmetry. The above structural analysis confirms that the rhombohedral and tetragonal phases coexist within the MPB region with $0.61 \le x \le 0.65$ and that a structural transformation from the rhombohedral to tetragonal phase occurs with increasing PT content. Therefore, with increasing PT content, the $(1-x)Ba(Sc_{1/2}Nb_{1/2})O_3-xPbTiO_3$ solid-solution system undergoes phase trans-

(18) Gao, L.; Huang, Y.; Hu, Y.; Du, H. *Ceram. Int.* **2007**, *33*, 1041.
(19) Zhang, X. D.; Kwon, D.; Kim, B. G. *Appl. Phys. Lett.* **2008**, *92*, 082906.
(20) Eitel, R. E.; Randall, C. A.; Shrout, T. R.; Rehrig, P. W.; Hackenberger, W.; Park, S.-E. *Jpn. J. Appl. Phys.* **2001**, *40*, 5999.
(21) Tinberg, D. S.; Trolier-McKinstry, S. *J. Appl. Phys.* **2007**, *101*, 024112.
(22) Huang, C.; Can, D. P. *J. Appl. Phys.* **2007**, *102*, 044103.
(23) Long, X.; Ye, Z.-G. *Chem. Mater.* **2007**, *19*, 1285.
(24) Politova, E. D.; Chuprakov, V. F. *Neorg. Mater.* **1985**, *21*, 473.

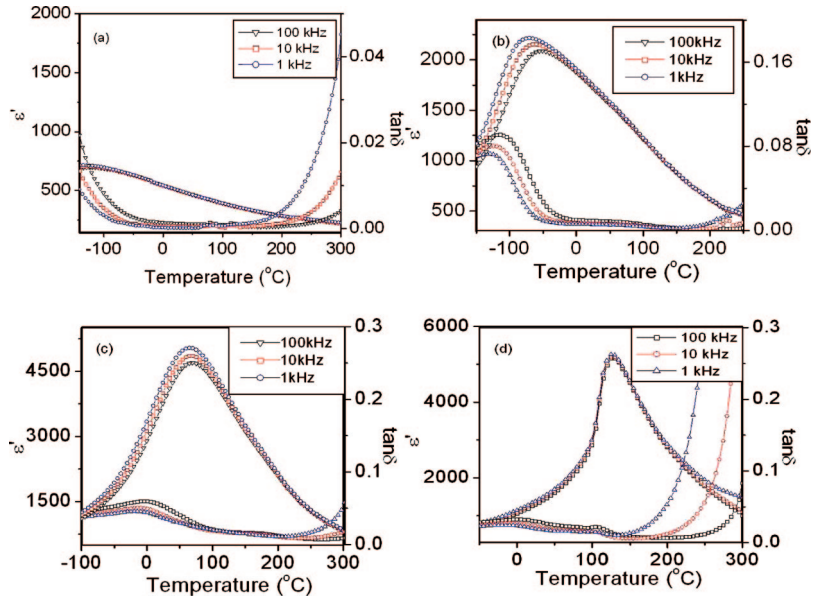

Figure 3. Temperature dependences of the dielectric constant (real permittivity, ε') and loss tangent (tan δ) of the $(1-x)Ba(Sc_{1/2}Nb_{1/2})O_3-xPbTiO_3$ ceramics with composition: (a) $x = 0.4$, (b) $x = 0.53$, (c) $x = 0.61$, and (d) $x = 0.65$, measured at 1, 10, and 100 kHz.

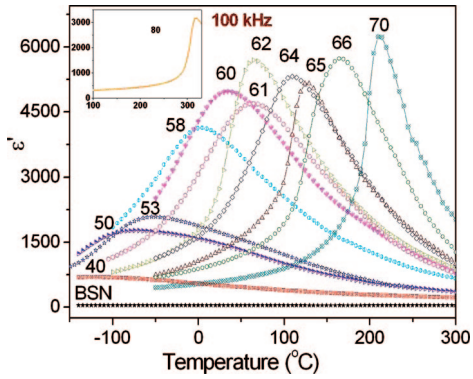

Figure 4. Dielectric constant of the $(1-x)Ba(Sc_{1/2}Nb_{1/2})O_3-xPbTiO_3$ ceramics ($x = 0$, 0.40, 0.50, 0.53, 0.58, 0.60, 0.61, 0.62, 0.64, 0.65, 0.66, 0.70, and 0.80) as a function of temperature measured at the frequency of 100 kHz.

formations from rhombohedral to (tetragonal + rhombohedral) (MPB) and then to tetragonal phases at room temperature.

3.2. Dielectric Properties. The temperature dependence of the dielectric constant (ε') of the $(1-x)Ba(Sc_{1/2}Nb_{1/2})O_3-xPbTiO_3$ ceramics were measured at different frequencies. Figure 3 shows the dielectric spectra of some selected compositions: $x = 0.40$, 0.53, 0.61, and 0.65. It can be seen that the behavior of dielectric constant depends closely on the composition x (PT content). For $x < 0.40$, the ε' maximum is low and no anomaly appears in the temperature range of −150 to 300 °C. The pure BSN is of rhombohedral symmetry and its dielectric constant is low with a quite flat temperature dependence (see Figure 4). Increasing the PT amount results in an increase in dielectric constant and the gradual appearance of a dielectric peak in its temperature dependence, which is enhanced with increasing PT cencentration. The 0.60BSN−0.40PT sample remains in the rhombohedral phase, but its dielectric constant is greatly enhanced because of the substitution of PT. For the samples with $x =$ 0.53−0.58, three interesting phenomena are noted: (a) the maximum dielectric constant value at room temperature increases sharply (from 2100 to 4150 at 100 kHz) with increasing PT content, (b) the temperature dependence of dielectric constant shows a broad maximum with frequency dispersion, and (c) the temperature of the dielectric maximum (T_{max}) shifts to higher temperature with increasing frequency, as shown in Figure 3b for $x = 0.53$. These phenomena indicate the characteristics of relaxor ferroelectric behavior for this composition range. For $x = 0.65$, the peak of dielectric constant becomes independent of frequency, suggesting normal ferroelectric properties with T_{max} becoming the ferroelectric Curie temperature T_C.[25−27] Therefore, with increasing PT amount, the BSN-PT solid solution exhibits a spectrum of interesting properties, from simple dielectric to relaxor ferroelectric and to normal ferroelectric.

Figure 4 shows the dielectric constant of the ceramic samples with $x = 0$, 0.40, 0.50, 0.53, 0.58, 0.60, 0.61, 0.62, 0.64, 0.65, 0.66, 0.70, and 0.80 as a function of temperature measured at the frequency of 100 kHz. It can be seen that, with increasing PT concentration, the dielectric peak becomes gradually sharper with reduced diffuseness as the system undergoes the above-mentioned transformation of dielectric behavior, and at the same time, T_{max} or T_c shifts to higher temperature (toward T_c of the pure PT).

Figure 5 presents the variation of the dielectric constant and loss tangent as a function of composition (x) measured at the frequency of 100 kHz at room temperature. It can be noted that the dielectric constant increases gradually with increasing PT content and reaches the maximum of about 5000, whereas the dielectric loss exhibits a minimum value of 0.005, in the vacinity of $x = 0.60$, which is just on the rhombohedral side of the MPB region. The dramatic enhancement of the dielectric properties can be directly attributed to the effects of chemical substitution of PT for BSN, which induces chemical disorder and polar nanoregions. The dynamics of polar nanoregions gives rise to the

(25) Dambekalne, M. J.; Borman, K. J.; Sternberg, A. R.; Gerdes, E.; Brante, I. V. *Izv. Akad. Nauk.* **1993**, *57*, 78.
(26) Bokov, A. A.; Ye, Z.-G. *J. Mater. Sci.* **2006**, *41*, 31.
(27) Ye, Z.-G. *Key Eng. Mater.* **1988**, *155*, 81.

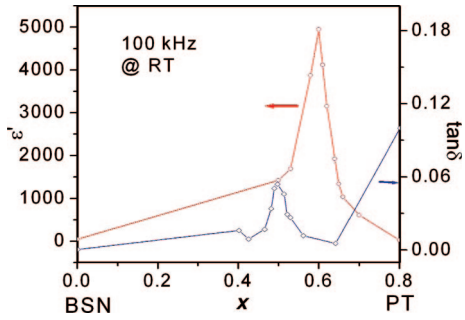

Figure 5. Variation of the room-temperature dielectric constant (ε') and loss tangent (tan δ) (at 100 kHz) of the $(1-x)Ba(Sc_{1/2}Nb_{1/2})O_3-xPbTiO_3$ ceramics as a function of composition.

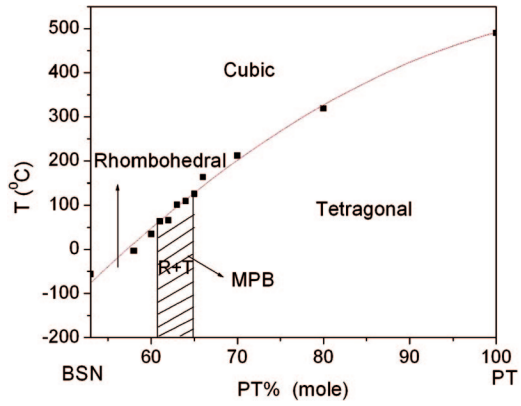

Figure 6. Solid-state phase diagram of the binary solid solution system of $(1-x)Ba(Sc_{1/2}Nb_{1/2})O_3-xPbTiO_3$.

relaxor behavior,[23] with the diffuse dielectric maximum turned around room temperature in those compositions. The high dielectric constant and low loss-tangent make the BSN-PT solid solution a promising candidate for such advanced dielectric applications as microwave dielectric components (resonance and filter) and high energy-density capacitors.

3.3. Phase Diagram. On the basis of the results of phase analysis by XRD and dielectric measurements, the morphotropic phase boundary (MPB) region and the Curie temperature (T_c) or maximum dielectric peak temperature (T_{max}) are obtained, and thereby the phase diagram of the BSN-PT binary solid solution system is established, as shown in Figure 6. The feature of the phase diagram is that a morphortropic phase boundary region exists in the composition range of $0.61 \le x \le 0.65$, where the rhombohedral phase and tetragonal phase coexist. It clearly shows that with increasing concentration of PT, the room-temperature phase transforms from the rhombohedral phase ($x < 0.61$) to a mixture of the rhombohedral and the tetragonal phases ($0.61 < x < 0.65$) and then to the tetragonal phase ($x \ge 0.65$). Compared with the BMN-PT system, which has the MPB in the range of $0.71 \le x \le 0.73$,[20] the MPB region of BSN-PT is broader and shifts to lower PT concentrations between $x = 0.61$ and $x = 0.65$.

3.4. Ferroelectricity. Figure 7 shows the polarization−electrical field ($P-E$) hysteresis loops of BSN-PT solid solution ceramics with compositions of $x = 0.40$, 0.61, 0.62, 0.63, 0.64, and 0.66 at a bipolar electric field of ±60 kV/cm. For $x = 0.40$, no hysteresis can be displayed, indicating a linear dielectric behavior. For $x \ge 0.61$, wide-open

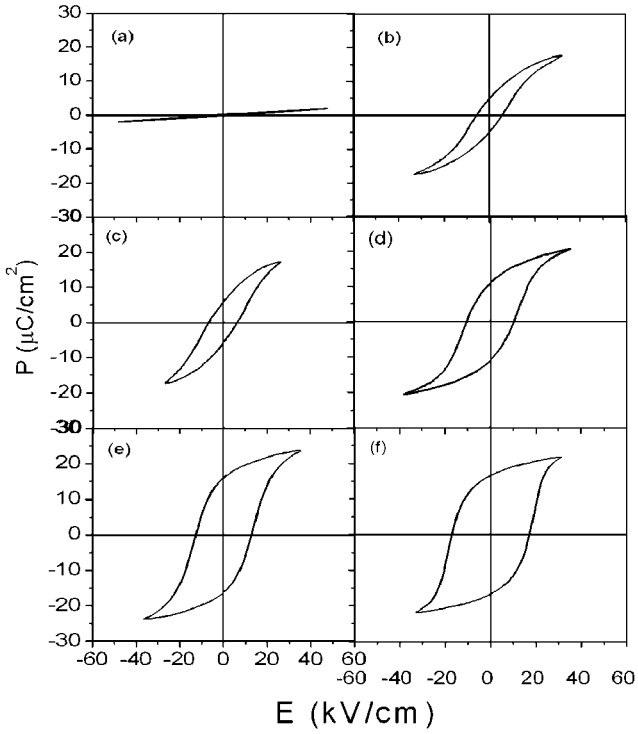

Figure 7. Polarization−electrical field ($P-E$) hysteresis loops of the $(1-x)Ba(Sc_{1/2}Nb_{1/2})O_3-xPbTiO_3$ ceramics with composition: (a) $x = 0.40$, (b) $x = 0.61$, (c) $x = 0.62$, (d) $x = 0.63$, (e) $x = 0.64$, and (f) $x = 0.66$ displayed at bipolar fields of about ±40 kV/cm.

hysteresis loops are displayed, indicating normal ferroelectricity with switchable macroscopic polarization. The remnant polarization (P_r) increases gradually with increasing PT concentration, reaching 11 μC/cm^2 for the ceramics of $x = 0.63$.

4. Conclusions

The perovskite solid solution $(1-x)Ba(Sc_{1/2}Nb_{1/2})O_3-xPbTiO_3$ ($0 \le x \le 1$) has been synthesized by solid-state reaction and the structural, dielectric and ferroelectric properties have been investigated. The solid-state phase diagram of the binary system has been established on the basis of the XRD structural analysis and temperature dependence of the dielectric properties, which delimits a morphortropic phase boundary region within the composition range of $0.61 \le x \le 0.65$ below a phase transition line between 50 and 125 °C, in which the rhombohedral phase of BSN origin coexists with the tetragonal phase of PT origin. In addition to the structural transformation, the chemical substitution of PT for BSN greatly affects the dielectric properties of the solid solution. At low PT contents, the solid solution behaves like a purely linear dielectric with low dielectric constant and flat temperature dependence, whereas the dielectric properties of the compositions with PT concentrations of $x = 0.53-0.58$ exhibit typical relaxor ferroelectric character with diffuse maxima shifting to higher temperatures at increasing frequencies. At higher PT concentrations, the solid solution shows normal ferroelectric behavior with open dielectric hysteresis loops. Therefore, as we across the composition range by increasing the PT content, the structure and properties of the $(1-x)$BSN−xPT solid solution at room

temperature undergo a series of interesting transformations: the crystal symmetry and phase component change from the rhombohedral phase to a mixture of the rhombohedral and the tetragonal phases, and then to the tetragonal phase, whereas the dielectric properties vary from purely liner dielectric to typical relaxor and then to normal ferroelectric behavior. It is also worth noting that the compositions close to the MPB region exhibit a high dielectric dielectric constant (∼5000 at 100 kHz) and low loss, making the BSN-PT solid solution promising material for prospective applications in microwave dielectric components and high-power-density capacitors.

Acknowledgment. This work was supported by the Key Project from FJIRSM (SZD08002), the Natural Science and Engineering Research Council of Canada (NERC) and the U.S. Office of Naval Research (Grant 00014-06-1-0166).

CM802734N